10-1-2015

# Small Molecule Inhibitor Design for Anaplastic Lymphoma Kinase Inhibition

Theodore D. Hansel
*Harvey Mudd College*

David J. Grabovsky
*Columbia University*

# Small Molecule Inhibitor Design for Anaplastic Lymphoma Kinase Inhibition

THEODORE D. HANSEL, DAVID J. GRABOVSKY

The Anaplastic Lymphoma Kinase (ALK) gene has been linked to tumorigenesis in a number of human cancers, including anaplastic large cell lymphoma (ALCL) and neuroblastoma. While ALK mutations in ALCL and many other cancers occur as a result of gene fusions with wild type kinase domains, those in neuroblastoma stem from single nucleotide polymorphisms (SNPs) in the kinase domain. These lead to autophosphorylation and constitutive signaling by ALK for cell growth and division, ultimately causing cancer. Crizotinib, an ATP-competitive ALK inhibitor, has proven to be an effective inhibitor of both $ALK^{WT}$ and $ALK^{Mutant}$ kinase domains, and is in the middle of clinical trials for neuroblastoma treatment. This review used the PyMOL and AutoDock Vina computational biology programs to predict the binding affinities of Crizotinib, Ceritinib (LDK378), and PF-922 to three different ALK kinase mutations in order to determine the most effective inhibitor. The EGFR inhibitors gefitinib and erlotinib were also analyzed in complex with ALK as negative controls to verify the specificity of the ALK inhibitors. The crystalline complexes were then qualitatively analyzed to uncover the mechanics behind the docking results. Based on the results generated by Vina, PF-922, representative of the second generation of ALK inhibitors, is predicted to be the most effective out of the tested compounds. These results may be used to predict the inhibitor that will require the lowest dosage to achieve the greatest inhibitory effect, hopefully leading to fewer side effects from treatment.

## Introduction

The Anaplastic Lymphoma Kinase (ALK) receptor tyrosine kinase has been implicated as a major oncogene in a variety of different cancers, ranging from adult non-small cell lung cancer (NSCLC) and anaplastic large-cell lymphoma (ALCL) to neuroblastoma in children[1]. The majority of these mutations are fusion proteins, such as NPM-ALK in ALCL[2] or EML4-ALK in NSCLC[3]. In these fusion proteins, the ALK kinase domain generally remains intact and wild type. However, ALK mutations in neuroblastoma are unique as they are frequently point mutations within the kinase domain. The mutations may be somatic or germline, with those causing tumorigenesis leading to constitutively active kinase domains[4]. Crizotinib is a dual ALK/MET inhibitor produced by Pfizer, and was one of the first ALK inhibitors introduced. Although first used with non-mutated (WT) ALK kinase domains in NSCLC, Crizotinib has also demonstrated efficacy preclinically in $ALK^{Mut}$ cell lines, and clinically in Phase I clinical trial patients[5].

For the purposes of this review, the PyMOL and AutoDock Vina computational programs were used to compare the binding affinity of Crizotinib with that of ATP, the natural ligand, as well as other ALK inhibitors. These other inhibitors include Ceritinib (LDK378) produced by Novartis, and a second-generation ALK inhibitor designed by Pfizer called PF-06463922 (PF-922). All of these inhibitors are ATP-competitive and function by binding preferentially to the ALK kinase domain and preventing ATP from entering the binding pocket, inhibiting the kinase activity. Theoretically, a higher binding affinity correlates with greater efficacy and reduced dosages to achieve the same inhibitory effect. *In vitro*, this effect would be shown by measuring ALK inhibition through western blotting or ELIZA assays. This review analyzes the binding affinities associated with each ligand, in addition to one designed for this study, for three different ALK point mutations. The first, C1097S, is used as a stand-in for the WT kinase domain found in ALK fusion proteins. This mutation stabilizes the model of the ALK kinase domain, and is found in all other models of the protein[6]. The R1275Q mutation represents the most common neuroblastoma mutation, while the F1174L mutation is the most resistant mutation commonly seen in the clinical setting[7].

## Methods

AutoDock Vina is a molecular docking program that takes in the molecular structures of a receptor and a ligand, runs computations simulating the ligand's docking into a specified binding pocket on the receptor, and predicts the ligand's binding affinity to its receptor[8]. Using

structures for the C1097S, R1275Q, and F1174L ALK mutations[6], as well as for each inhibitor[9–11], a docking analysis in Vina for each ligand-receptor pairing was run to determine binding affinities for each pairing. Vina also produces files containing the ligand's docked pose responsible for the reported affinity; these files were opened in the PyMOL molecular viewer and analyzed qualitatively in terms of their conformations.

Before running Vina, special .pdbqt files describing each molecule involved in docking were prepared. PDB files (descriptions of the spatial arrangement and types of atoms in a molecule) containing each compound's structure were downloaded from pdb.org and isolated in PyMOL. $ALK^{WT}$ was downloaded in complex with a piperidine-carboxamide inhibitor[6], which was removed; the other two ALK mutations were downloaded in apo[6] (ligand-free) form. All three drugs (Crizotinib, Ceritinib, and PF-922) were originally downloaded in complex with ALK[9–11], which was subsequently removed from each ligand.

Each ligand file was then opened in AutoDockTools (ADT), a GUI extension of Vina, and subsequently saved in .pdbqt format, which preserves the atom locations specified in PDB format, but also gives each atom partial charges (q) and an AutoDock-specific atom type (t). The same was done with each receptor; however, crystallographic water molecules were removed and polar hydrogens were added (as preferred by Vina) before saving each file in .pdbqt format. The final step in molecule preparation involved defining a search space on the receptors where Vina would search for a binding pocket. Each protein was visually inspected in ADT until the binding site was found; the search space was then specified as a box around the binding site, with ($x$, $y$, $z$) coordinates for its center and $x$, $y$, and $z$-lengths for its sides.

Once the .pdbqt files for all receptors and proteins were saved, a configuration (config) file was written and Vina was run. The config file gave Vina the filenames of the ligand and receptor to be docked, as well as the coordinates and size of the search space box found graphically in ADT. (See Appendix A for the format and parameters of the config file.) Vina was run from a Windows command prompt: after changing the computer's directory to the folder where vina.exe was located, the command

```
"\Vina\vina.exe" --config conf.txt --log log.txt
```

read the config file and created a log of its output as the analysis ran.

Vina's output takes the form of .pdbqt files containing each ligand's 9 most likely docking poses, as well as the log of the 9 affinities corresponding to those poses. The .pdbqt files were saved for visualization and comparative analysis, and only the highest affinity for each docking run, representing the ligand's most likely pose, was recorded. Because Vina uses a random seed for each docking run, its results are nondeterministic; the program must therefore run several times for each ligand-receptor pairing to produce reliable data. Affinities from 10 docking runs were recorded in a Microsoft Excel spreadsheet and then averaged to produce each pairing's mean affinity.

## Results: Computational Analysis

Figures 1 – 5 below summarize the results of our study, listing each ligand's binding affinities to all three proteins (A), followed by images of the ligands docked with each of the three versions of ALK: C1097S (B), R1275Q (C), and F1174L (D). Figure 1 shows data on ATP, Figure 2 on Crizotinib, Figure 3 on Ceritinib, Figure 4 on PF-922, and Figure 5 on TDH-01, a drug designed by one of the authors based on the structure of PF-922.. Comparison of the ligands bound to $ALK^{WT}$ shows that PF-922 (Figure 4 (B)) and TDH-01 (Figure 5 (B)) both had the highest affinity, followed by Crizotinib (Figure 2 (B)), Ceritinib (Figure 3 (B)), and finally ATP (Figure 1 (B)). Binding affinities associated with both mutated proteins exhibited the same order, with PF-922 pulling slightly ahead of TDH-01. In every simulation, ATP was the weakest binding partner. Another table summarizing our results, which compares ligands instead of proteins, can be found in Appendix B.

Comparison of the receptors yielded less obvious patterns. ATP bound to $ALK^{WT}$ (Figure 1 (B)) with a lower affinity than to $ALK^{F1174L}$ (Figure 1 (D)), but with higher affinity than to $ALK^{R1275Q}$ (Figure 1 (C)). Crizotinib did not follow this trend, binding weakest to $ALK^{R1275Q}$ (Figure 2 (C)), slightly stronger to $ALK^{F1174L}$ (Figure 2 (D)), and strongest to $ALK^{WT}$ (Figure 2 (B)), for which it was designed. Ceritinib behaved differently, binding to $ALK^{R1275Q}$ (Figure 3 (C)) with higher affinity than to $ALK^{F1174L}$ (Figure 3 (D)); yet still the bond was not as strong as to $ALK^{WT}$ (Figure 3 (B)). PF-922, the overall best ALK inhibitor, interestingly bound with higher affinity to $ALK^{Mut}$ proteins (Figure 4 (C-D)) than to $ALK^{WT}$ (Fiure 4 (B)). TDH-01 also fared better with mutated proteins (Figure 5 (C-D)) than with $ATP^{WT}$ (Figure 5 (A)), actually binding best to the notoriously resistant $ALK^{F1174L}$ (Figure 5 (D)). These trends in PF-922 and TDH-01 show their functional similarity, as well as their specificity for mutated ALK variants.

A

| ALK Mutation Status | Average Binding Affinity (kcal/mol) |
|---|---|
| C1097S | 6.81 |
| R1275Q | 6.39 |
| F1174L | 6.94 |

B

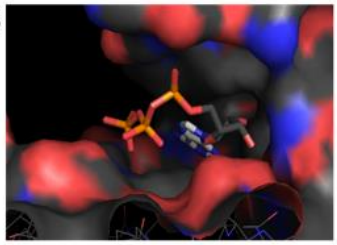

C

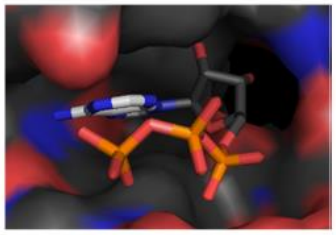

D

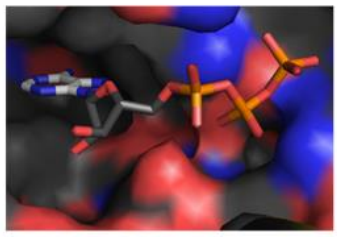

Figure 1

A

| ALK Mutation Status | Average Binding Affinity (kcal/mol) |
|---|---|
| C1097S | 8.19 |
| R1275Q | 7.92 |
| F1174L | 7.99 |

B

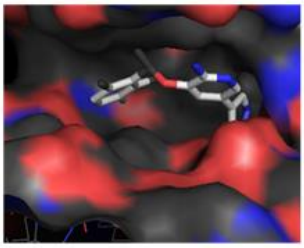

C

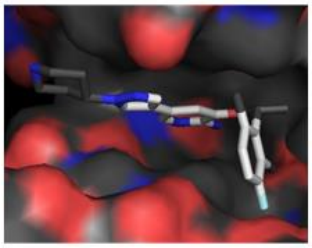

D

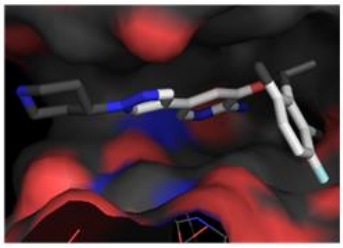

Figure 2

A

| ALK Mutation Status | Average Binding Affinity (kcal/mol) |
|---|---|
| C1097S | 7.9 |
| R1275Q | 7.51 |
| F1174L | 7.43 |

B

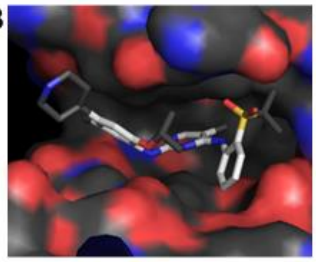

C

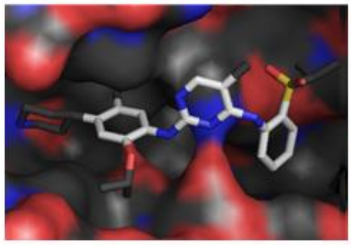

D

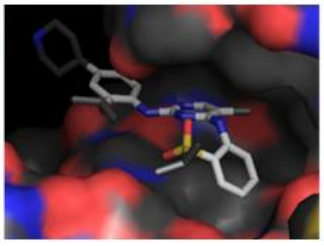

Figure 3

A

| ALK Mutation Status | Average Binding Affinity (kcal/mol) |
|---|---|
| C1097S | 9.2 |
| R1275Q | 10.4 |
| F1174L | 10.4 |

B

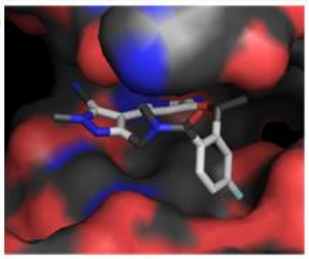

C

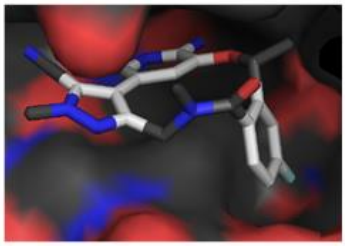

D

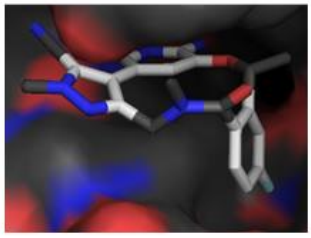

Figure 4

A

| ALK Mutation Status | Average Binding Affinity (kcal/mol) |
|---|---|
| C1097S | 9.2 |
| R1275Q | 9.7 |
| F1174L | 10.1 |

B

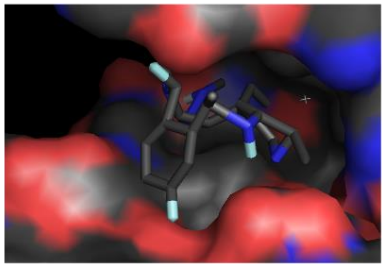

C

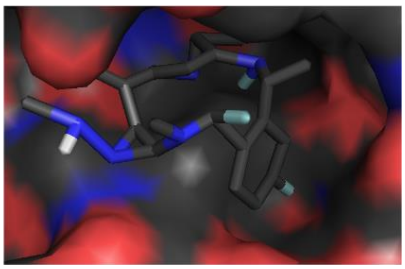

D

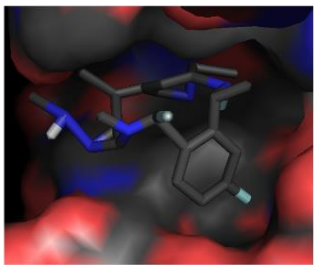

Figure 5

## Qualitative Comparison

The binding affinity between a protein and its ligand are a direct result of how tightly the ligand fits into its binding pocket, as well as how well the ligand matches "hot spots" in the pocket. Hot spots are regions in the protein of high electrical charge that can create strong intermolecular forces to hold the ligand inside the binding site. As previously noted, all of the inhibitors demonstrated a greater binding affinity than ATP for all ALK mutations, which is necessary for the inhibitor to function. By analyzing the crystal structure of the inhibitors in complex with the ALK kinase domain, it becomes clear that the more effective compounds, such as PF-922, TDH-01, and Crizotinib, bind more preferably than Ceritinib or ATP.

Figure 1 (B) shows the crystalline structure of ATP in the WT kinase domain. The fit of the molecule inside the pocket is relatively loose, and there are only a few hotspots linked to electronegative regions in the molecule. These explain the relatively low binding affinity. There are even some electronegative regions of the molecule near negative hotspots, which would suggest repulsion. These same principles are also evident in $ALK^{R1275Q}$ in figure 1 (C) and $ALK^{F1174L}$ in figure 1 (D). Crizotinib, shown in complex with $ALK^{WT}$ in figure 2 (B), has a similar linear structure to that of ATP, but features a highly electronegative fluorine attached to an aromatic ring, giving it the ability to bind with a hot spot in the pocket ATP was unable to reach, likely giving Crizotinib its preferential affinity. Crizotinib also binds strongly to this hotspot in both $ALK^{R1275Q}$ (figure 2 (C)) and $ALK^{F1174L}$ (figure 2 (D)). Ceritinib also binds more preferentially than ATP to all three ALK mutations (Figure 3). Since Ceritinib does not appear to directly bind with many hot spots, its increased affinity is likely due to a tighter fit than ATP's, although it also features a linear structure similar to ATP and Crizotinib but lacks the highly interactive fluorine.

PF-922, representing the second generation ALK inhibitors, displays the highest binding affinity out of all of the reviewed inhibitors (figure 4 (A)). Like Crizotinib, it features the aromatic ring-linked fluorine to strongly bind to hot spots, but departs from the linear design in favor of a ringed shape. Resulting in an altogether wider molecule in the main horizontal plane, PF-922 fits more snugly into the binding pocket than the other inhibitors, allowing it gain a stronger affinity to the walls of the pocket while interacting with particular hotspots (figure 4 (B-D)).

TDH-01 was designed by one of the authors based on the PF-922 geometry, and attempted to gain a higher binding affinity than PF-922 by creating more regions of high electronegativity in the molecule. While TDH-01 interacted with many of the same hot spots as PF-922 and had a nearly identical docking pose, the additional electronegativity also increased its repulsion of the binding pocket's negatively charged regions. While also present in $ALK^{WT}$ and $ALK^{F1174L}$ (figure 5 (D)), this is especially evident with the proximity of the anterior nitrogen atoms and the negative region of $ALK^{R1275Q}$ (figure 5 (C)). Figure 6 below is a side-by-side comparison of the structures of PF-922 (A) and TDH-01 (B). The increased polarity within TDH-01, as evidenced by the abundance of fluorine, nitrogen, and oxygen atoms, is most likely liable for its slight decrease in binding affinity.

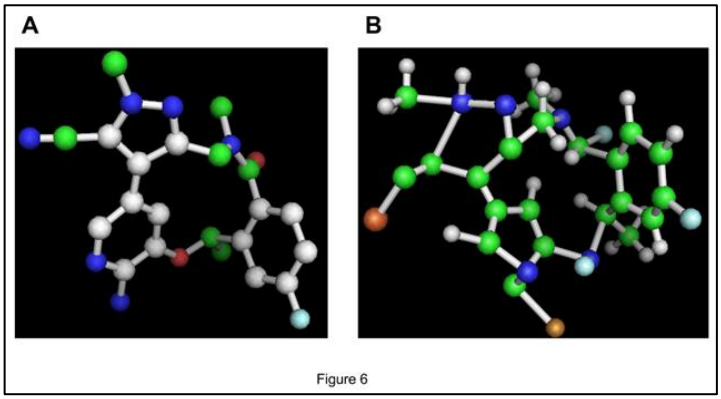

Figure 6

## Discussion and Conclusion

Based on our results, PF-922 is predicted to be the most effective ALK inhibitor, especially for the resistant F1174L mutation. Our data matches that of other published studies[9]. Additionally, the protein models accurately reflect the observed *in vitro* resistance of the F174L ALK mutation due to its increased ATP binding affinity[12]. This review has demonstrated the beneficial effect of not only conformational compatibility, but also hotspot targeting in rational drug design. The inhibitors that demonstrated the highest binding affinities were those with the greatest amount of conformity to the pocket and those which targeted the most hotspots.

The most obvious path for future research is preclinical and clinical testing of these compounds. Crizotinib has already proven its efficacy in the clinical setting, and the other drugs are also ambling in this direction. TDH-01, at present only a theoretical model, would have to be produced in the laboratory prior to any bench testing. While direct clinical or preclinical comparisons of these compounds are unlikely, this review

serves as a good basis for the comparison of ALK inhibitor efficacy from computational and qualitative perspectives. Computational results gathered during preclinical testing of new compounds allows researchers to better focus on testing drugs with higher chances of success, allowing for more efficient use of limited research funding. The current process for drug design (high throughput screening) is not only laborious, but also incredibly expensive. By integrating data gathered through computational methods, pharmaceutical engineers may more intelligently create drugs, streamlining the development and production of more effective novel treatments.

---

## References


1. Available at: http://www.cellsignet.com/learn/papers/Ardini. Accessed December 1, 2014.
2. Zdzalik D, Dymek B, Grygielewicz P, et al. Activating mutations in ALK kinase domain confer resistance to structurally unrelated ALK inhibitors in NPM-ALK-positive anaplastic large-cell lymphoma. J Cancer Res Clin Oncol. 2014;140(4):589-98.
3. Wang Y, Wang S, Xu S, Qu J, Liu B. Clinicopathologic Features of Patients with Non-Small Cell Lung Cancer Harboring the EML4-ALK Fusion Gene: A Meta-Analysis. PLoS ONE. 2014;9(10):e110617.
4. Mossé YP, Laudenslager M, Longo L, et al. Identification of ALK as a major familial neuroblastoma predisposition gene. Nature. 2008;455(7215):930-5.
5. Mossé YP, Lim MS, Voss SD, et al. Safety and activity of crizotinib for paediatric patients with refractory solid tumours or anaplastic large-cell lymphoma: a Children's Oncology Group phase 1 consortium study. Lancet Oncol. 2013;14(6):472-80.
6. Epstein LF, Chen H, Emkey R, Whittington DA. The R1275Q neuroblastoma mutant and certain ATP-competitive inhibitors stabilize alternative activation loop conformations of anaplastic lymphoma kinase. J Biol Chem. 2012;287(44):37447-57.
7. Carpenter EL, Mossé YP. Targeting ALK in neuroblastoma--preclinical and clinical advancements. Nat Rev Clin Oncol. 2012;9(7):391-9.
8. Seeliger D, de Groot BL. Ligand docking and binding site analysis with PyMOL and Autodock/Vina. *Journal of Computer-Aided Molecular Design* 2010;24(5):417-422. doi:10.1007/s10822-010-9352-6.
9. Johnson TW, Richardson PF, Bailey S, Brooun A, Burke BJ, Collins MR, Cui JJ, Deal JG, Deng YL, Dinh D, Engstrom LD, He M, Hoffman J, Hoffman RL, Huang Q, Kania RS, Kath JC, Lam H, Lam JL, Le PT, Lingardo L, Liu W, McTigue M, Palmer CL, Sach NW, Smeal T, Smith GL, Stewart AE, Timofeevski S, Zhu H, Zhu J, Zou HY, Edwards MP. Discovery of (10R)-7-amino-12-fluoro-2,10,16-trimethyl-15-oxo-10,15,16,17-tetrahydro-2H-8,4-(metheno)pyrazolo[4,3-h][2,5,11]-benzoxadiazacyclotetradecine-3-carbonitrile (PF-06463922), a macrocyclic inhibitor of anaplastic lymphoma kinase (ALK) and c-ros oncogene 1 (ROS1) with preclinical brain exposure and broad-spectrum potency against ALK-resistant mutations. Journal of Medicinal Chemistry 2014. 12;57(11):4720-44.
10. Cui JJ, Tran-dubé M, Shen H, et al. Structure based drug design of crizotinib (PF-02341066), a potent and selective dual inhibitor of mesenchymal-epithelial transition factor (c-MET) kinase and anaplastic lymphoma kinase (ALK). J Med Chem. 2011;54(18):6342-63.
11. Friboulet L, Li N, Katayama R, et al. The ALK inhibitor ceritinib overcomes crizotinib resistance in non-small cell lung cancer. Cancer Discov. 2014;4(6):662-73.
12. Bresler SC, Wood AC, Haglund EA, et al. Differential inhibitor sensitivity of anaplastic lymphoma kinase variants found in neuroblastoma. Sci Transl Med. 2011;3(108):108ra114.


## Bibliography


- Available at: http://pubs.acs.org/doi/abs/10.1021/ci100039k. Accessed December 1, 2014.
- Akbar H, Cancelas J, Williams DA, Zheng J, Zheng Y. Rational design and applications of a Rac GTPase-specific small molecule inhibitor. Meth Enzymol. 2006;406:554-65.
- Available at: http://www.sciencedirect.com/science/article/pii/S096089 94X1400331X. Accessed December 1, 2014.
- Available at: http://www.scripps.edu/florida/technologies/hts/. Accessed December 1, 2014.
- Available at: http://www.informedicalcme.com/lucatoday/crizotinib-story-from-target-to-fda-approval/. Accessed December 1, 2014.

- Available at: http://www.guidetopharmacology.org/GRAC/LigandDisplayForward?ligandId=1713 Accessed November 9, 2014.
- Available at: http://www.guidetopharmacology.org/GRAC/LigandDisplayForward?ligandId=7476. Accessed November 9, 2014.
- Available at: http://www.guidetopharmacology.org/GRAC/LigandDisplayForward?ligandId=7397. Accessed November 9, 2014.
- Available at: http://www.guidetopharmacology.org/GRAC/LigandDisplayForward?ligandId=4903. Accessed November 9, 2014.


## Acknowledgements


The authors would like to thank the Mossé Laboratory at the Childhood Cancer Center at the Children's Hospital of Philadelphia for their review of these findings and their guidance on background information related to the Anaplastic Lymphoma Kinase. Members of the Mossé laboratory did not perform this research or write any portion of this article.


## Funding


There was no funding for this project. PyMOL and AutoDock Vina were obtained free under educational use licenses, while the free WebMO demo server was used to create TDH-01.


## Appendix A: The Configuration File

```
receptor = filename.pdbqt
ligand = filename.pdbqt

out = out.pdbqt

center_x = 20.0
center_y = 15.0
center_z = variable:
      C1097S: 63
      R1275Q: 10
      F1174L: 11

size_x = 20
size_y = 20
size_z = 20

exhaustiveness = 8
```

## Appendix B: Average Inhibitor Binding Affinities

Inhibitors

| (kcal/mol) | ATP | Ceritinib | Crizotinib | PF-922 | TDH-01 |
|---|---|---|---|---|---|
| **C1097S** | 6.81 | 7.9 | 8.19 | 9.20 | 9.20 |
| **R1275Q** | 6.39 | 7.51 | 7.92 | 10.40 | 9.70 |
| **F1174L** | 6.94 | 7.43 | 7.99 | 10.40 | 10.10 |

Negative Controls

| (kcal/mol) | Gefitinib | Erlotinib |
|---|---|---|
| **C1097S** | 7.61 | 6.55 |
| **R1275Q** | 7.22 | 6.66 |
| **F1174L** | 7.50 | 6.65 |

*Note: All binding affinities listed above and in Figures 1 – 5 are given in terms of the energy released as binding occurs.*